HHS Public Access

Author manuscript

Placenta. Author manuscript; available in PMC 2019 June 01.

Published in final edited form as:

Placenta. 2018 June ; 66: 74–81. doi:10.1016/j.placenta.2018.05.001.

Understanding abnormal uterine artery Doppler waveforms: a novel computational model to explore potential causes within the utero-placental vasculature

Alys R CLARK, PhD[1], **Joanna L JAMES, PhD**[2], **Gordon N STEVENSON, DPhil**[3], and **Sally L COLLINS, BMBCh, DPhil, MRCOG**[4]

[1]Auckland Bioengineering Institute, University of Auckland, New Zealand [2]Department of Obstetrics and Gynaecology, Faculty of Medical and Health Sciences, University of Auckland, New Zealand [3]School of Women's & Children's Health, University of New South Wales, Sydney, Australia [4]Nuffield Department of Obstetrics & Gynaecology, University of Oxford, and the Fetal Medicine Unit, John Radcliffe Hospital, Oxford, United Kingdom

Abstract

Introduction: Uterine artery (UtA) Doppler indices are one of the most commonly employed screening tests for pre-eclampsia worldwide. Abnormal indices appear to result from increased uterine vascular resistance, but anatomical complexity and lack of appropriate animal models mean that little is known about the relative contribution of each of the components of the uterine vasculature to the overall UtA Doppler waveform. Previous computational models suggested that trophoblast-mediated spiral artery remodeling has a dominant effect on the UtA Doppler waveform. However, these models did not incorporate the myometrial arterio-venous anastomoses, which have significant potential to affect utero-placental haemodynamics.

Methods: We present a more anatomically complete computational model, explicitly incorporating a structural description of each component of the uterine vasculature, and crucially including myometrial arterio-venous anastomoses as parallel pathways for blood-flow away from the placental bed. Wave transmission theory was applied to the network to predict UtA waveforms.

Results: Our model shows that high UtA resistance indices, combined with notching, reflect an abnormal remodelling of the entire uterine vasculature. Incomplete spiral artery remodelling alone is unlikely to cause abnormal UtA Doppler waveforms as increased resistance in these arteries can be 'buffered' by upstream anastomoses. Critically, our results indicate that the radial arteries, may have a more important effect on utero-placental flow dynamics, and the UtA Doppler waveform than previously thought.

Conclusions: This model suggests that to appropriately interpret UtA Doppler waveforms they must be considered to be reflecting changes in the entire system, rather than just the spiral arteries.

Corresponding Author: Dr Alys R Clark, Auckland Bioengineering Institute, The University of Auckland, Private Bag 92019, Auckland 1142, New Zealand, Phone: +64 (0) 93737599 ext 85604, Fax: +64 (0) 9 3677157.

AUTHOR CONTRIBUTIONS

All authors designed research; A. R. Clark developed software required to perform research; A. R. Clark, J. L. James, G. Stevenson, S. L. Collins parameterized model. A. R. Clark analysed data; A. R. Clark, J. L. James, G. Stevenson, S. L. Collins wrote the paper.

INTRODUCTION

Pre-eclampsia contributes significantly to the global burden of adverse maternal and neonatal outcomes [1]. Pre-eclampsia and eclampsia alone account for 1 in 7 maternal deaths worldwide [1], equivalent to as many as 60 000 maternal deaths annually [2]. High resistance changes in uterine artery (UtA) Doppler waveforms have been used to try to predict pre-eclampsia since the 1980s [3]. For such an established clinical diagnostic technique, surprisingly little is known as to why changes observed in the waveform occur. Increased understanding of underlying mechanisms could potentially improve the predictive value of this simple, non-invasive tool. Current belief is that a deficiency in remodeling of the terminal part of the arterial network (the spiral arteries, SAs) produces greater resistance to flow and manifests as increased 'upstream' vessel impedance[4]. The SAs are unique in that they are colonized and actively remodeled by trophoblast from tightly coiling, highly muscular vessels to wide funnel like openings to the surface of the placenta [5]. This dominance of SAs in determining UtA resistance indices was supported by studies showing poor trophoblast-induced remodeling of the SAs correlating with high UtA resistance indices [6–9], reinforced by computational modelling which grouped the entire utero-placental vasculature as a single load impedance [10, 11]. However, the UtA waveform cannot be just a function of trophoblast-induced SA remodeling, as it changes during the menstrual cycle, with contraceptive devices, pharmacological agents and in abdominal pregnancies where the SAs are not exposed to trophoblasts [12–17]. Furthermore, no significant changes in the UtA waveform are observed immediately after placental delivery when the SAs abruptly close, most likely because blood flow is redirected through an arterio-venous (A-V) anastomotic network in the myometrium [18]. This suggests that other uterine vessels may have an important influence on the UtA waveform. Indeed, when the larger uterine vessels and a myometrial resistance are incorporated into a model, UtA notching appeared to be associated with high uterine or arcuate artery compliance [19].

Since seminal models in the field were first derived, increased evidence of the structural extent, and functional importance of A-V anastomoses within the myometrium, has arisen [18]. This A-V network acts as a parallel pathway to uterine blood flow, allowing it to bypass the placenta, and has been hypothesized to act as a means to modulate uterine resistance by protecting the fetus against maternal hypertensive events [18]. To date, no model has represented the full utero-placental vascular anatomy, nor quantified the relative contribution of each downstream vessel to the UtA waveform including these anastomoses. To understand how each uterine vasculature component affects the UtA waveform, an anatomically complete model was developed to predict UtA waveforms.

MATERIALS AND METHODS

A model of the utero-placental circulation accounting explicitly for the size and compliance of all levels of uterine vasculature is proposed, and wave transmission theory applied to the network to predict UtA waveforms.

Geometric representations of UtA structure

The bilateral uterine arteries branch from the internal iliac arteries (Fig. 1). Arcuate arteries arise from the UtA and run parallel to the uterine surface (Fig. 1a). They branch into radial arteries, which give rise to the SAs. The SAs feed the intervillous space (IVS) and undergo significant trophoblast-induced remodeling in the first trimester from tortuous vessels into wide bore conduits (Fig. 1b). Myometrial A-V anastomoses provide an alternative pathway for blood (Fig. 1b), and are believed to regulate pressure in the IVS in pregnancy [20]. As the UtA waveform does not change when the SAs clamp shut upon placental delivery [18], A-V anastomoses must be capable of carrying almost all the blood-flow through a term placental bed (600–700 ml/minute) yet they have not been included in any previous computational models of uterine flow.

We consider two new models of the uterine circulation (Fig. 2) compared to the classical lumped transmission line model of Mo et al. [10, 11]. The classical model groups the entire vasculature distal to the UtA (arcuate, radial and SAs, and the IVS) as a single load impedance, assuming the primary site of resistance in the uterine circulation is the terminal SAs, which dominate load impedance [10, 11]. Here, Model 1 considers the terminal load impedance to represent the resistance and compliance of only the SAs and IVS, and includes A-V anastomoses explicitly as an alternative pathway for blood-flow. The model also includes explicit structural representations of arcuate and radial arteries as described in the literature. Model 2 represents the anatomy immediately post-delivery, when the IVS has been removed and the SAs closed, but radial, arcuate and UtA structure remains dilated to the late-pregnancy state.

Arterial dimensions

Limited quantitative data exist on the uterine vasculature structure during pregnancy. However, estimates can be made for all arterial dimensions from the literature. When dimensions are uncertain they are varied to assess the implications of assuming a single value for vessel length/diameter in the model.

Uterine artery: The radius of the UtA at mid-gestation is assumed to be 2mm [10, 21] and total UtA length to be 10cm [10, 11]. Typically the point of insonation is <2 cm from the uterus,[9] and 1cm below the UtA bifurcation based on prior work (Fig. 2) [10, 11].

Arcuate arteries: The arcuate arteries distend throughout pregnancy, by 12 weeks they show some sign of dilation, and by 20 weeks have larger radius than the UtA [21]. At term they are comparable in size to the internal iliac artery (and twice that of the proximal UtA, which is uncommon in circulatory systems) [21]. The length of a typical UtA segment (between radial artery branches) can be extrapolated from the non-pregnant state based on analysis by Farrer-Brown et al. [22] and Talbert. [19] The length of an average arcuate artery on is assumed to be 90cm, and 1000 radial arteries are assumed to be fed by 20 arcuate arteries [19]. Thus, an average segment of arcuate artery between branches is assumed to be 18.0mm long.

Radial arteries: The radial arteries are described as opened coils at 21 weeks of gestation [19, 23], and branch to supply the myometrium and endometrium. Their diameter has been measured at 0.30–0.35mm at physiological filling pressures in normal pregnancies [24]. Following Talbert [19] we assume 50 radial arteries per arcuate artery. A-V anastomoses occur at the junctional zone of the myometrium, which is the distal 4mm of the muscle [25]. Total myometrial thickness at 20 weeks of gestation is estimated to be 10mm [26]. Therefore, we estimated the length of a radial artery before it gives rise to the A-V anastomoses to be ~6mm.

A-V anastomoses: Few studies have estimated A-V anastomosis dimensions. However, microsphere studies suggest a radius $r_{a\text{-}v}$=0.2mm is likely (the default model parameter [25]), and anatomical studies suggest up to 2–3mm in diameter, in post-delivery specimens [18]. For completeness we assessed model predictions for $r_{a\text{-}v}$ from 0.0mm (no anastomoses) to 1.5mm [18]. The model is insensitive to $r_{a\text{-}v}$ >0.5mm. We assume anastomosis length of ~9mm (half the distance between two radial arteries, as the anastomoses branch from radial arteries to uterine veins).

Spiral arteries and IVS: As in previous models, a terminal load impedance represents the distal uterine vasculature and the IVS, with the IVS as the ground. The distal vasculature is therefore represented as a resistor in parallel to a capacitor [11]. The resistor represents the resistance of the distal uterine vasculature to flow, assumed to be dominated by the combined resistance the SAs and IVS. The capacitor represents their compliance, which can impose a delay in the reflected waveform. The resistance component can be derived from estimates of total utero-placental resistance (2.49 Pa.s/mm^3) after deducting the resistance of the upstream circulation. Using spiral artery dimensions derived by Burton et al. [4] this results in a spiral artery contribution of approximately 60% the total terminal load impedance at term, with the remainder due to resistance to flow in the IVS.

Vascular impedance

Flow propagation in the uterine circulation is described using ‘transmission line’ theory, which uses an electrical analogue approach to describing blood-flow in a vascular network [10, 11, 27]. Relevant mathematical methods are provided as supplementary material. The implementation of the model is publicly available, scripted in Python (https://github.com/ABI-Rep-Dev-Group/network-wave-transmission.git).

Incident flow waveform: The incident flow waveform is defined at the intersection between the internal iliac artery and the UtA. This point is assumed far enough from the clinical point of measurement (where the UtA crosses the external iliac artery) to have constant shape, so its relative amplitude and phase is unaffected by changes in the utero-placental vasculature in pregnancy [11]. This can be demonstrated clinically [3]. The measured flow waveform at the insonation site is then predicted. The absolute flow rate through the system is a function of its resistance (assuming a constant pressure drop) thus as the system is perturbed, flow rate is scaled in proportion to resistance. Mo et al. [11] defined the harmonics of a normal UtA Doppler waveform at 20 weeks of gestation. Using this waveform, and Model 1 parameterized exactly to the classical model [11], we calculated the

incident flow waveform required to produce the same harmonics at the insonation site. For all subsequent simulations, we held the incident flow waveform fixed, except for a constant scaling, and predicted insonation site flow/pressure waveforms.

RESULTS

Following implementation, models were validated against published physiological and mathematical data. At the insonation site at baseline, the predicted ratio of systolic (S) to diastolic (D) flow velocity S/D=1.85, resistance index RI=(S-D)/S=0.46, and pulsatility index PI=(S-D)/mean velocity=0.64 were consistent with previous modelling studies [10, 11, 19], and nomograms of Doppler indices in the second and third trimesters of pregnancy [28, 29].

A-V anastomoses mitigate the impact of SA resistance on UtA Doppler waveforms:

A-V anastomoses provide an alternative parallel pathway for blood to flow through the uterus, which reduces the resistance of the uterine vasculature, compared with the case where no A-V anastomoses are included in the model (Fig. 3A). A-V anastomoses also reduce the impact of elevated SA resistance on UtA waveforms, as when SA resistance is high, blood is diverted through the A-V anastomoses and does not reach the IVS (Fig. 3B–C). When a single 0.1mm radius anastomosis connects each radial artery directly with a vein (bypassing the IVS), increases in SA resistance have significantly less effect on RI, PI and S/D than in the absence of anastomoses, although high SA resistance does induce notching in the UtA waveform (Fig 4). A 0.4–0.5mm radius anastomosis, akin to anatomical observations, allows normal velocity profiles for up to 10-fold increase in SA resistance (Fig. 4). Thus, when A-V anastomoses are taken into account, physiological increases in SA and/or IVS resistance do not drastically alter Doppler waveforms, suggesting other uterine vessels must contribute to abnormal Doppler waveforms seen in pregnancy pathologies.

Radial arteries of reduced caliber can cause high resistance indices and notching: The predicted impact of radial artery radius on UtA velocity waveforms is small for radii >0.15mm. However, below this threshold value the model predicts rapid increases in PI, RI and S/D and dicrotic notching, even with normal SA resistance (Fig. 5). Radial arteries in pre-eclamptic women have reduced lumen diameter (~0.11mm at physiological filling pressures [24]). At this pathological radius, the model predicts dicrotic notching and abnormally high indices (S/D=4.73, RI=0.78, PI=1.87) even in the absence of elevated SA resistance. Baseline estimates of radial artery radius (0.25mm) reflect the remodeled mid- to late-pregnancy state. The higher resistance waveforms seen prior to 20 weeks of gestation could reflect the relatively small caliber of radial arteries. As pregnancy progresses, PI decreases, and a notch often seen early in pregnancy disappears by mid to late gestation, which our model predicts is consistent with increased radial artery caliber. Taken together, these data suggest that inadequate dilation of the radial arteries can result in abnormal Doppler waveforms without concurrent increased SA resistance. Thus, the radial arteries may play a more important role in the pathogenesis of pregnancy disorders than previously considered.

Post-delivery function: After the placenta is delivered the uterus immediately contracts providing a 'living ligature' to the placental bed by pinching off the terminal SAs. If SA resistance was the predominant contributor to increased RI, PI and S/D seen in pregnancy pathologies, complete closure of these vessels should dramatically increase these indices. However, Schaaps et al. [18] demonstrated no change in the uterine waveform following delivery. When the SAs/IVS are removed from the model, all blood that is delivered to the uterus travels through the A-V anastomoses, equivalent to the post-delivery state, with the largest arteries in the uterine vasculature dilated as in pregnancy but not feeding the placenta. The model predicts normal low resistance uterine Doppler profiles in the absence of the placenta, provided that the entire uterine vasculature is normally dilated, and that the equivalent radius of shunt pathways arising from the radial arteries is >0.5mm (well within the range demonstrated in anatomical studies [18], Fig. 6). In this case S/D=1.66, RI=0.40 and PI=0.55. Post-partum 'low resistance' waveforms can therefore be explained by normal arterial dilation through the uterus and the presence of A-V anastomoses. As the entire uterine vasculature decreases in caliber to a pre-pregnancy state during puerperium typical non-pregnant 'high resistance' features of the velocity waveform are predicted to return. As multiparous women typically have larger uterine arteries than primiparous women, this return to a 'high resistance' state may not exactly reflect pre-pregnancy waveforms. Abnormal, 'high resistance' UtA waveforms that persist post-partum must be due to incomplete radial artery dilation or a sparse A-V shunt network.

DISCUSSION

In this study, a computational model of UtA blood-flow dynamics was presented, and an investigation into how structural perturbations to the utero-placental circulation lead to changes in UtA Doppler waveforms conducted. Unlike previous models, each component of the uterine vasculature, including the A-V anastomosis networks in the myometrium [18], was explicitly modeled.

The model's predictions are consistent with previous models of the UtA waveform via three specific analyses: 1) In comparison to normal anatomical values, halving the radius of the uterine and arcuate arteries increases the RI=0.80, PI=1.61 and S/D=5.05, but does not induce a notch [10, 19]. 2) Dicrotic notching with elevated RI can occur with elevated compliance in the arcuate and uterine arteries in pregnancy, without changes in SA resistance [10]. 3) A higher than normal arcuate/uterine compliance can mask the increased diastolic slope in Doppler waveforms that has been interpreted previously as increased placental bed resistance [19].When A-V anastomoses are not considered (as in previous models), increases in SA resistance result in decreased volumetric blood-flow (for a given driving pressure) and increased RIs. Notching appears once SA resistance reaches 3x its baseline value (Figs. 3A and 4a)) [10, 11].

The anastomotic network is hypothesized to function as a shunt, protecting against acute hypertensive events [18], and modulating blood pressure in the IVS to avoid placental damage [18, 20, 30]. A parallel A-V anastomosis network is shown by the model to reduce total uterine vascular resistance, allowing significant increases in uterine blood-flow through gestation. The presence of A-V anastomoses with dimensions observed in late pregnancy

can entirely explain normal low resistance waveforms observed in the days post-partum (Fig. 6). The reversal of UtA remodeling and decrease in the extent of A-V anastomoses over several weeks post-partum is also consistent with our model returning to a high resistance waveform with notching. The model predicts that the A-V anastomosis network mitigates the impact of high SA resistance on UtA Doppler waveforms. Indeed, although an abnormal UtA waveform is correlated with inadequate trophoblast colonization of the SAs, S/D is normal in more than half of women with impaired trophoblast colonization [31]. Abnormal S/D and impaired trophoblast colonization leads to worse prognosis than normal S/D despite impaired trophoblast colonization [31]. Thus, if inadequate SA remodeling is not a requirement for pathological UtA impedance, and if A-V anastomoses are capable of mitigating SA resistance during pregnancy, this raises an important question about which aspects of the uterine vasculature directly contribute to clinically measured pathological increases in resistance indices and/or the presence of a notch in pathological pregnancies.

Our model directly addresses this question by quantitatively assessing the impact of each component of the uterine vasculature on UtA waveforms. Whilst SA remodeling has an important role in ensuring that maternal blood perfuses evenly through the IVS [4], the elevated resistance indices and/or notching seen clinically most likely represents inadequate dilation of the larger uterine vessels. This model demonstrates, that it is the radial arteries not the terminal SA which have the largest contribution to the waveform. Radial arteries are small diameter vessels, and without significant dilation would remain narrower than remodeled SAs. Our model predicts that undilated radial arteries can simultaneously result in notching and elevated resistance, even with normal SA remodeling. Radial artery lumen diameters seen in pre-eclampsia [24] are sufficiently small for our model to predict both high resistance indices and UtA notching. The transformation of both SA and radial arteries in pregnancy may be functionally intertwined, thus it is likely that abnormal UtA waveforms relate to inadequate SA remodeling along with inadequate arterial dilation upstream of the SAs. This relationship may be causative, with trophoblast-mediated remodeling extending from the SAs to the proximal portions of the radial arteries [5, 32], and/or a result of initial inadequate proximal arterial dilation affecting the extent of the downstream SA remodeling [4]. Alternatively, there may be a shared mechanistic driver for both SA remodeling and radial artery dilation from vascular priming or preconditioning [33], from endocrine factors such as estrogen, or from uterine immune cells which play key roles in priming SAs for trophoblast-induced remodeling as well as initiating outward vascular remodeling in other tissues [34–36].

Talbert [19], in the first study to apply detailed anatomical measurements of the uterine vasculature in a computational model, attributed notching and high resistance indices primarily to abnormally high UtA compliance, which was ground-breaking in its predictions that high SA/IVS resistance is unlikely to be the primary contributor to notch presence [37]. The time-domain model presented by Talbert is mathematically different to the frequency domain model presented here but uses similar principles to solve iteratively for blood pressure and flow rates. As with the Talbert model, pressure and flow profiles can be derived from our model results at any location in the uterine vasculature. Despite methodological differences our model predicts similar impacts of each anatomic feature presented in this prior study, and thus not all results of this prior study are repeated here. In particular, our

model agrees that high UtA compliance results in notching. As poorly remodeled vessels have increased muscle tone, one would expect an increased compliance in these cases. Studies have shown systemic endothelial dysfunction, and a failure of the systemic maternal vasculature to adapt to pregnancy is a feature in pre-eclampsia [38–40] and FGR [41]. However, it is not clear whether this is a cause or consequence of the pathology, or whether systemic vascular function translates to uterine vessels [41].

The uterine circulation is not alone in containing an extensive network of anastomoses or shunt pathways, that may actively or passively be recruited in times of elevated blood flow or pressure [42]. Similar anastomosis networks potentially play a role is in the lung vasculature, where anastomoses are suggested to also play a role in protecting an exchange surface against hypertensive events [43]. However, these anastomotic networks are almost universally neglected in computational models of vascular physiology, and interpretation of clinical metrics of vascular resistance. The model presented here highlights the importance of parallel pathways in determining total vascular resistance, and in the context of the uterine vasculature suggests that anastomoses could be protective against maternal hypertension, but also could mask the impact of micro-vascular pathology on observed features of flow in larger arteries.

Model limitations:

Our model includes structural data on the size and connectivity of the uterine vascular network, but is necessarily simplified, due to sparsity of quantitative structural data regarding the uterine vasculature. Our model was parameterized using fixed values of structural characteristics such as vessel length, radius, and number. However, all structural parameters were varied to assess their impact on model predictions, and the most significant contributors were presented. The model at baseline was parameterized to a population mean, and individual factors such as maternal heart rate, blood pressures neglected, all of which vary between individuals and can be impacted by maternal age, weight and by pathology. The model could be more closely parameterized to an individual using maternal hemodynamic data (e.g. heart rate and blood pressure) and histopathology data on changes in uterine artery dimensions across populations. Indeed histology analysis from hysterectomy sections from the Boyd collection have recently demonstrated the extent of radial and arcuate artery dilation and the possible role of the radial arteries in regulating uteroplacental blood flow early in gestation [44]. Although the model is not patient specific, it clearly indicates the importance of considering the role of the complete uterine vasculature in interpreting UtA waveforms.

Similarly, variation within an individual with regard to SA remodeling is neglected from the model, for example, asymmetric SA remodeling (central versus peripheral) in the same placenta. The theory employed could be extended to include variable extent of anastomosis frequency or SA/IVS resistance within an individual, however, it is unlikely to significantly influence trends in model predictions. The model assumes branch angle and curvature are insignificant, which may impact flow resistance and distribution. For example, an approximately 90^{o} branching angle to A-V anastomoses may reduce the volumetric flow diverted to these pathways, however, analysis of blood oxygen content by Schaaps et al. [18]

suggests blood transit through these pathways is significant and occurs in volumes consistent with model predictions. Future studies should focus on determining precise vessel sizes/numbers at each anatomical location by using histology, along with emerging imaging technologies such as microbubble ultrasound [44, 45]. This would provide more detailed structural and functional data to be incorporated into a model of this type.

CONCLUSIONS

Our model predicts that A-V anastomoses play a significant role in determining UtA hemodynamics, allowing for the persistence of low resistance waveforms post-partum and mitigating the impact of SA resistance on the waveform. This data suggests that UtA Doppler waveforms are determined by the structure of the entire uterine vasculature, with high resistance radial arteries potentially playing a larger role in determining UtA waveforms than previously considered. The classical interpretation that this waveform directly reflects the degree of resistance in the distal SAs is impacted upon by the extent of shunting, and is potentially 'buffered' if extensive A-V anastomoses are present. The proximal uterine vasculature, particularly the radial arteries, should not therefore be overlooked as major contributors to utero-placental hemodynamic function.

Supplementary Material

Refer to Web version on PubMed Central for supplementary material.

ACKNOWLEDGEMENTS

Sources of funding are Royal Society of New Zealand Marsden Fund (13-UOA-032, Clark/James), Royal Society of New Zealand Rutherford Discovery Fellowship (14-UOA-019, Clark), Eunice Kennedy Shriver National Institute of Child Health and Human Development (NICHD) Human Placenta Project of the National Institutes of Health under award number UO1 HD 087209 and the Leslie Stevens' Fund (Collins/Stevenson). The funders of this research had no role in study design, analysis of data, writing of report or decision to submit the article for publication.

Funding Sources

Royal Society of New Zealand Marsden Fund (13-UOA-032, Clark/James), Royal Society of New Zealand Rutherford Discovery Fellowship (14-UOA-019, Clark), Eunice Kennedy Shriver National Institute of Child Health and Human Development (NICHD) Human Placenta Project of the National Institutes of Health under award number UO1 HD 087209 and the Leslie Stevens' Fund (Collins/Stevenson).

REFERENCES

1. Say L, et al., Global causes of maternal death: a WHO systematic analysis. Lancet Glob Health, 2014 2(6): p. e323–33. [PubMed: 25103301]
2. American College of, O., Gynecologists, and P. Task Force on Hypertension in, Hypertension in pregnancy. Report of the American College of Obstetricians and Gynecologists' Task Force on Hypertension in Pregnancy. Obstet Gynecol, 2013 122(5): p. 1122–31. [PubMed: 24150027]
3. Cohen-Overbeek T, Pearce JM, and Campbell S, The antenatal assessment of utero-placental and feto-placental blood flow using Doppler ultrasound. Ultrasound Med Biol, 1985 11(2): p. 329–39. [PubMed: 3898503]
4. Burton GJ, et al., Rheological and physiological consequences of conversion of the maternal spiral arteries for uteroplacental blood flow during human pregnancy. Placenta, 2009 30(6): p. 473–82. [PubMed: 19375795]

5. James J, Chamley L, and Clark A, Feeding your baby in utero: How the uteroplacental circulation impacts pregnancy Physiology, 2017 32(3): p. 234–245. [PubMed: 28404739]
6. Guzin K, et al., The relation of increased uterine artery blood flow resistance and impaired trophoblast invasion in pre-eclamptic pregnancies. Arch Gynecol Obstet, 2005 272(4): p. 283–8. [PubMed: 16007505]
7. Sagol S, et al., The comparison of uterine artery Doppler velocimetry with the histopathology of the placental bed. Aust N Z J Obstet Gynaecol, 1999 39(3): p. 324–9. [PubMed: 10554944]
8. Olofsson P, Laurini RN, and Marsal K, A high uterine artery pulsatility index reflects a defective development of placental bed spiral arteries in pregnancies complicated by hypertension and fetal growth retardation. Eur J Obstet Gynecol Reprod Biol, 1993 49(3): p. 161–8. [PubMed: 8405630]
9. Prefumo F, Sebire N, and Thilaganathan B, Decreased endovascular trophoblast invasion in first trimester pregnancies with high-resistance uterine artery Doppler indices. Hum Reprod, 2004 19(1): p. 206–209. [PubMed: 14688183]
10. Adamson S, et al., Effect of placental resistance, arterial diameter, and blood pressure on the uterine arterial velocity waveform: a computer modelling approach. Ultrasound in Medicine and Biology, 1989 15(5): p. 437–442. [PubMed: 2675446]
11. Mo L, et al., A transmission line modelling approach to the interpretation of uterine doppler waveforms. Ultrasound in Medicine and Biology, 1988 14(5): p. 365–376. [PubMed: 3051611]
12. Collins S, et al., Abdominal pregnancy: A perfusion confusion? Placenta, 2011 32: p. 793–795. [PubMed: 21839509]
13. Acácio G, Uterine artery Doppler patterns in abdominal pregnancy. Ultrasound Obstet Gynecol, 2002 20: p. 194–196. [PubMed: 12153673]
14. Steer CV, et al., Transvaginal colour flow imaging of the uterine arteries during the ovarian and menstrual cycles. Hum Reprod, 1990 5(4): p. 391–5. [PubMed: 2193940]
15. Jarvela I, Tekay A, and Jouppila P, The effect of a levonorgestrel-releasing intrauterine system on uterine artery blood flow, hormone concentrations and ovarian cyst formation in fertile women. Hum Reprod, 1998 13(12): p. 3379–83. [PubMed: 9886518]
16. Jimenez MF, et al., The effect of the levonorgestrel-releasing intrauterine system and the copper intrauterine device on subendometrial microvascularization and uterine artery blood flow. Fertil Steril, 2008 90(5): p. 1574–8. [PubMed: 18191844]
17. Hale SA, et al., Sildenafil increases uterine blood flow in nonpregnant nulliparous women. Reprod Sci, 2010 17(4): p. 358–65. [PubMed: 20228381]
18. Schaaps J-P, et al., Shunting in the intervillous space: New concepts in uteroplacental vscularization. American Journal of Obstetrics and Gynecology, 2005 192: p. 323–332. [PubMed: 15672043]
19. Talbert D, Uterine flow velocity waveform shape as an indicator of maternal and placental development failure mechanisms: A model-based synthesising approach. Ultrasound in Obstetrics and Gynecology, 1995 6: p. 261–271. [PubMed: 8590189]
20. Gyselaers W and Peeters L, Physiological implications of arteriovenous anastomoses and venous hemodynamic dysfunction in early gestational uterine circulation: A review. The Journal of Maternal-Fetal and Neonatal Medicine, 2013 26(9): p. 841–846. [PubMed: 23339488]
21. Fernstrom I, Arteriography of the uterine artery. Acta Radiologica, 1955 Suppl 122: p. 66–83.
22. Farrer-Brown G, Beilby J, and Tarbit M, The blood supply of the uterus. 1. Arterial vasculature. The Journal of Obstetrics and Gynaecology of the British Commonwealth, 1970 77(8): p. 673–681. [PubMed: 5452128]
23. Burchell R, et al., Vascular anatomy of the human uterus and pregnancy wastage. British Journal of Obstetrics and Gynaecology, 1978 85(698–706).
24. Ong S, et al., Remodelling of the myometrial radial arteries in preeclampsia. American Journal of Obstetrics and Gynecology, 2005 192(2): p. 572–579. [PubMed: 15696005]
25. Heckel G and Tobin C, Arteriovenous shunts in the myometrium. American Journal of Obstetrics and Gynecology, 1956 71(1): p. 199–205. [PubMed: 13282989]
26. Degani S, et al., Myometrial thickness in pregnancy: Longitudinal sonographic study. J Ultrasound Med, 1998 17: p. 661–665. [PubMed: 9771611]

27. Zhu Y, et al., Transmission line models to simulate the impedance of the uterine vasculature during the ovarian cycle and pregnancy. European Journal of Obstetrics & Gynecology and Reproductive Biology, 2009 144S: p. S184–S194.
28. Gómez O, et al., Reference ranges for uterine artery mean pulsatility index at 11–41 weeks of gestation. Ultrasound in Obstetrics and Gynecology, 2008 32: p. 128–132. [PubMed: 18457355]
29. Trudinger B, Giles W, and Cook C, Uteroplacental blood flow velocity-time waveforms in normal and complicated pregnancy. British Journal of Obstetrics and Gynaecology, 1985 92: p. 39–45. [PubMed: 3966989]
30. Saghian R, et al., Journal of Biomechanical Engineering, Association of placental jets and mega-jets with reduced villous density.
31. Lin S, et al., Uterine artery Doppler velocimitry in relation to trophoblast migration in the myometrium of the placental bed. Obstet Gynecol, 1995 85: p. 760–765. [PubMed: 7724109]
32. Brosens I, Robertson W, and Dixon H, The physiological response ofthe vessels of the placental bed to normal pregnancy. The Journal of Pathology, 1967 93(2): p. 569–579.
33. Brosens J, et al., A role for menstruation in preconditioning the uterus for successful pregnancy. American Journal of Obstetrics and Gynecology, 2009 200(615): p. e611–616.
34. de Ziegler D, Bessis R, and Frydman R, Vacular resistance of uterine arteries: Physiological effects of estradiol and progesterone. Fertility and Sterility, 1991 55: p. 775–779. [PubMed: 2010003]
35. Jauniaux E, et al., Influence of human chorionic gondaotrophin, oestradiol and progesterone on uteroplacental and corpus luteum blood flow in normal early pregnancy. Human Reproduction, 1992 7: p. 1467–1473. [PubMed: 1291579]
36. Xiao D, et al., Direct effect of steroid hormones in attenuating uterine arterial myogenic tone: role of protein kinase x/extra-cellular signal related kinase ½. Hypertension, 2009 54: p. 352–258. [PubMed: 19528364]
37. Campbell, The uteroplacental circulation - why computer modelling makes sense. Ultrasound in Obstetrics and Gynecology, 1995 6: p. 237–239. [PubMed: 8590185]
38. Bird IM, Zhang L, and Magness RR, Possible mechanisms underlying pregnancy-induced changes in uterine artery endothelial function. American Journal of Physiology - Regulatory, Integrative and Comparative Physiology, 2003 284(2): p. R245–R258.
39. Mahdy Z, et al., The responsiveness of isolated human hand vein endothelial cells in normal pregnancy and in pre-eclampsia. The Journal of Physiology, 1998 508(Pt 2): p. 609–617. [PubMed: 9508821]
40. Myatt L and Webster RP, Vascular biology of preeclampsia. Journal of Thrombosis and Haemostasis, 2009 7(3): p. 375–384. [PubMed: 19087223]
41. Yinon Y, et al., Vascular dysfunction in women with a history of preeclampsia and intrauterine growth restriction. Insights Into Future Vascular Risk, 2010 122(18): p. 1846–1853.
42. Mellander S and Johansson B, Control of resistance, exchange and capacitance functions in the peripheral circulation. Pharmalogical Reviews, 1968 20(3): p. 117–196.
43. Eldridge M, et al., Exercise induced intrapulmonary arteriovenous shunting in healthy humans. Journal of Applied Physiology, 2004 97: p. 797–805. [PubMed: 15107409]
44. Roberts V, et al., Early first trimester uteroplacental flow and the progressive disintegration of spiral artery plugs: new insights from contrast-enhanced ultrasound and tissue histopathology. Hum Reprod, 2017 32(12): p. 2382–2393. [PubMed: 29136193]
45. Roberts V, et al., Quantitative assessment of placental perfusion by contrast-enhanced ultrasound in macaques and human subjects. Am J Obstet Gynecol, 2016 214(3): p. 369.e1–369.e8. [PubMed: 26928151]

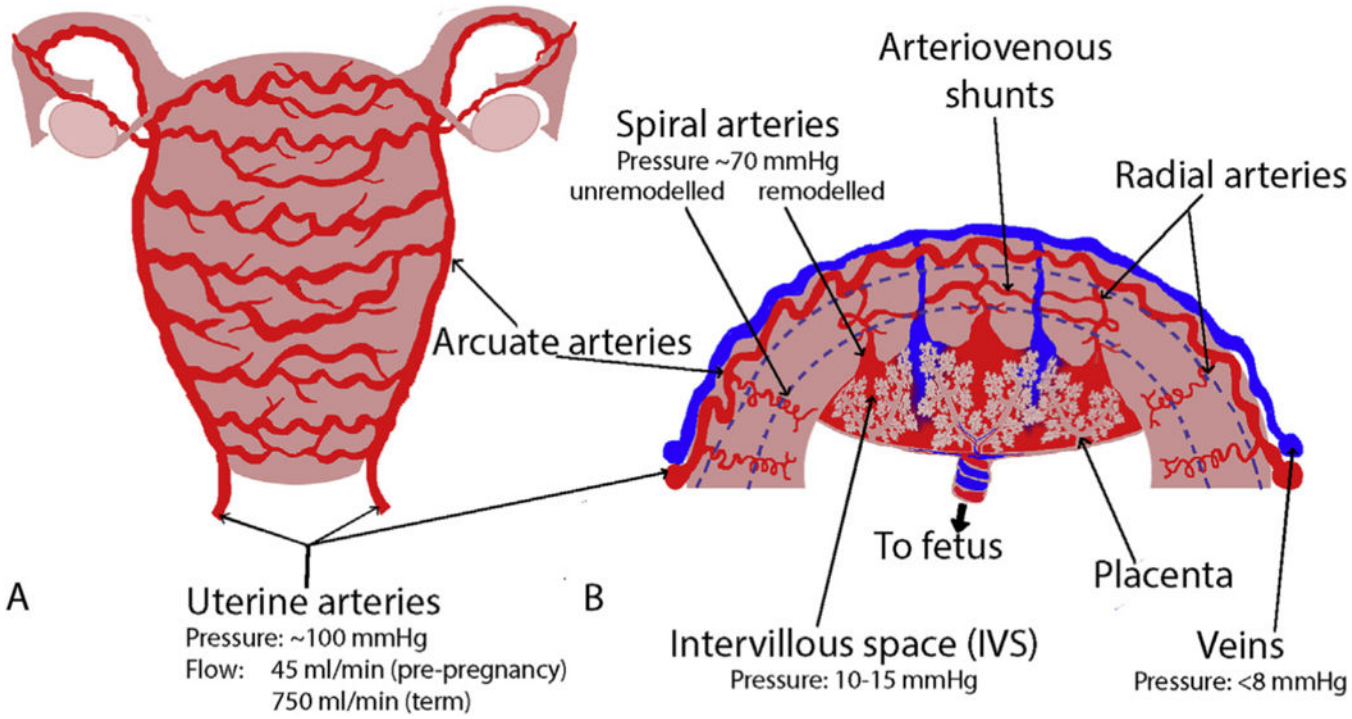

Figure 1:

A schematic of the structure of the uterine vasculature in pregnancy. Blood is primarily delivered to the uterus via the uterine arteries, which branch to the arcuate arteries. The arcuate arteries traverse the uterus in “horizontal rings” (Panel A). The arcuate arteries then branch through the walls of the uterus to radial, basal and spiral arteries, which in pregnancy deliver maternal blood to the site of the placenta where it bathes the placental structures in the intervillous space (Panel B). There are also arterio-venous (A-V) anastomoses (shunt pathways) that connect myometrial radial arteries to the venous side of the uterine vasculature. These anastomoses potentially carry the majority of uterine blood-flow post-delivery. The blue dotted lines in B approximately delineate the myometrium from the endometrium in the placental bed, and the myometrium from the perimetrium near the surface of the uterus.

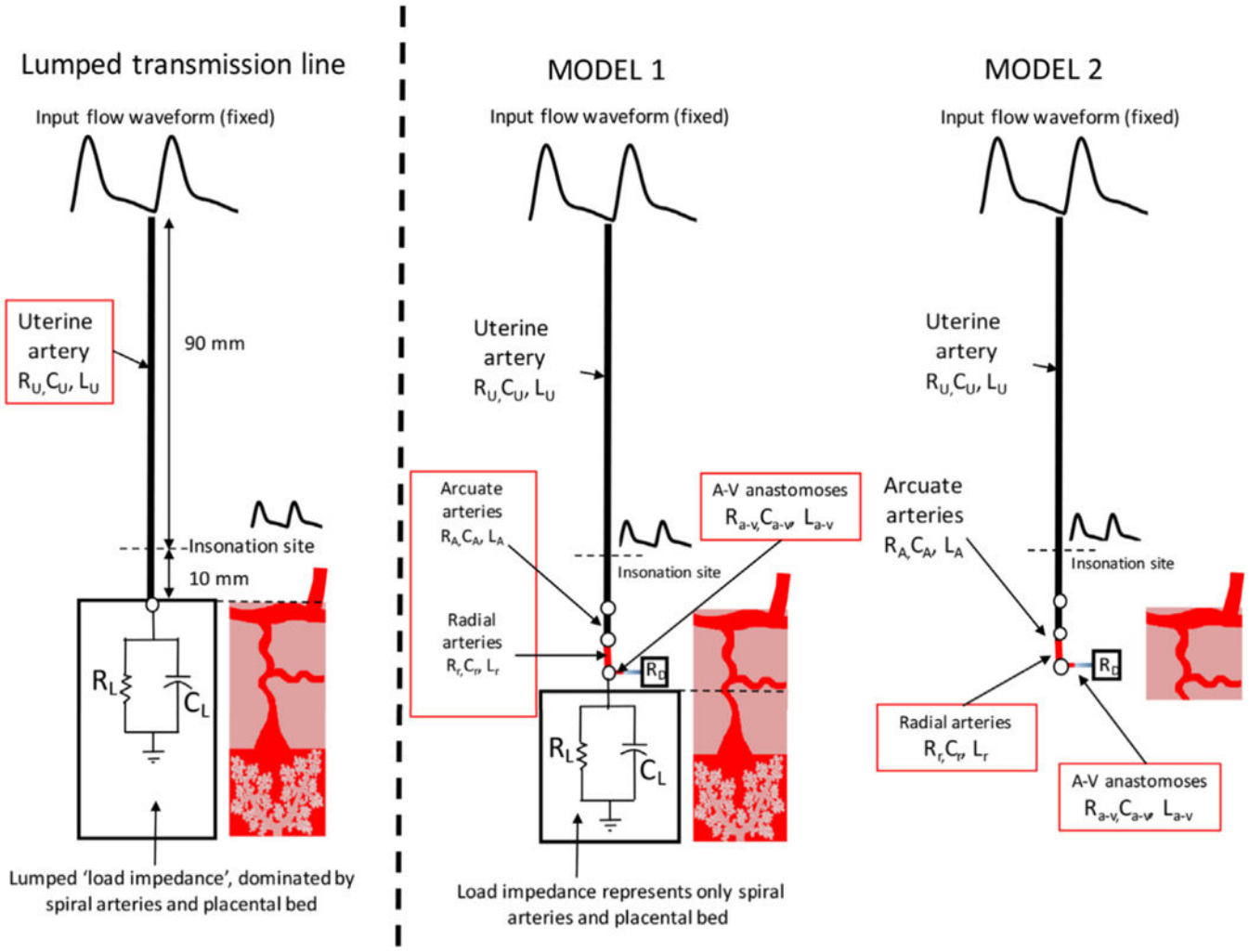

Figure 2:

The model representations of the uterine arteries used in this study, compared with the previous transmission line model of Mo et al. (10,11). Model 1 explicitly incorporates the arcuate arteries, radial arteries and the arterio-venous (A-V) anastomoses that connect the uterine arteries and veins and are assumed to carry the entire uterine blood-flow post-pregnancy. Model 2 represents the post-pregnancy state. Each arterial segment explicitly included in the model is assigned a resistance, a compliance and an inductance, based on their structural characteristics.

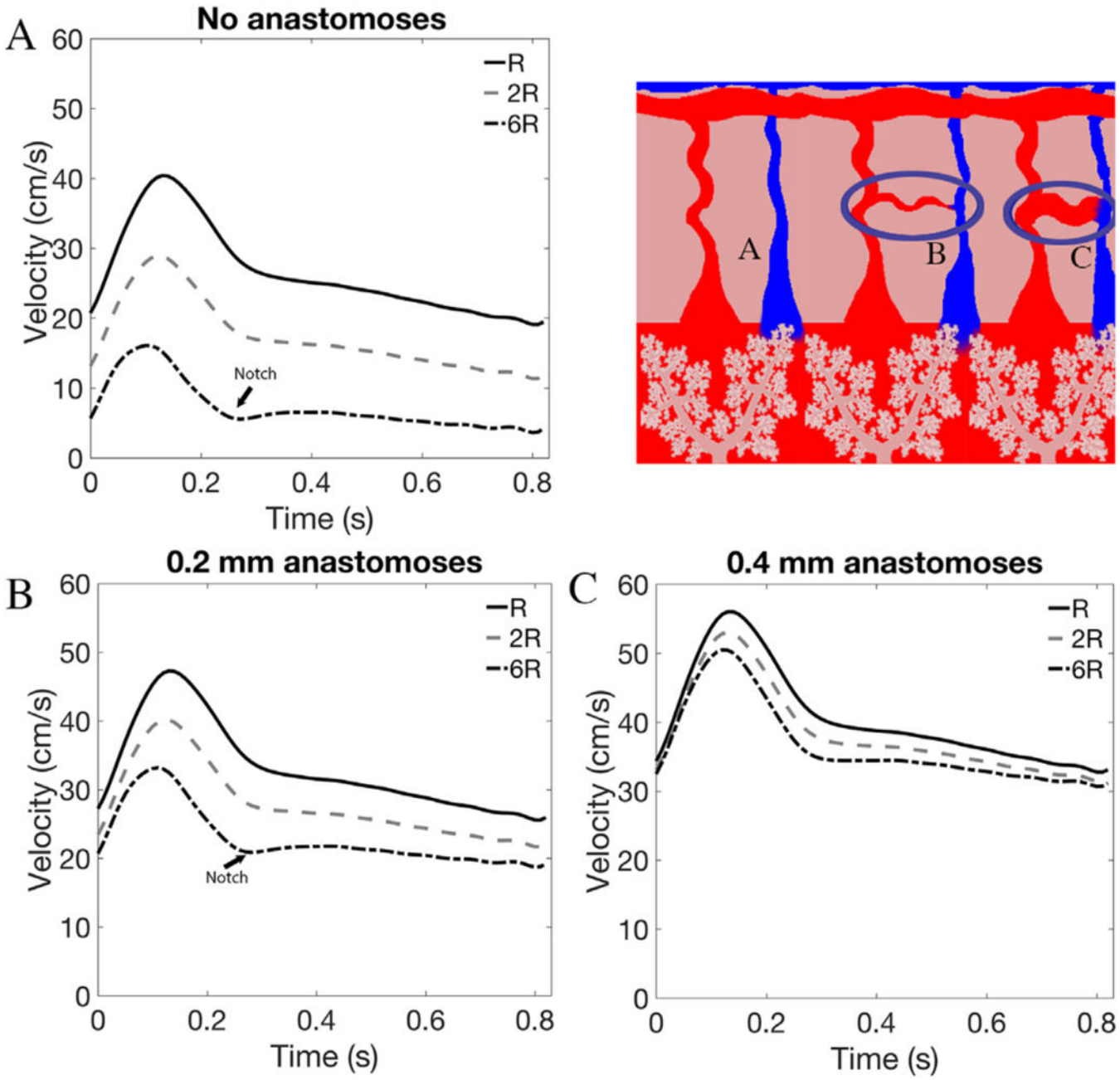

Figure 3:

The impact of anastomosis presence and structure on model predictions. Panel A shows model predictions of uterine artery velocity waveforms for increasing spiral artery resistance (R) with no A-V anastomoses included in the model. As R increases to two- and six-times baseline values there is a significant decrease in system resistance and a dicrotic notch forms. Panels B and C show model predictions of uterine artery velocity waveforms for increasing R in the presence of 0.2 and 0.4mm radius anastomoses. These anastomoses provide a parallel pathway for blood-flow away from the placental, thus mitigating the impact of increased spiral artery resistance on uterine artery waveforms.

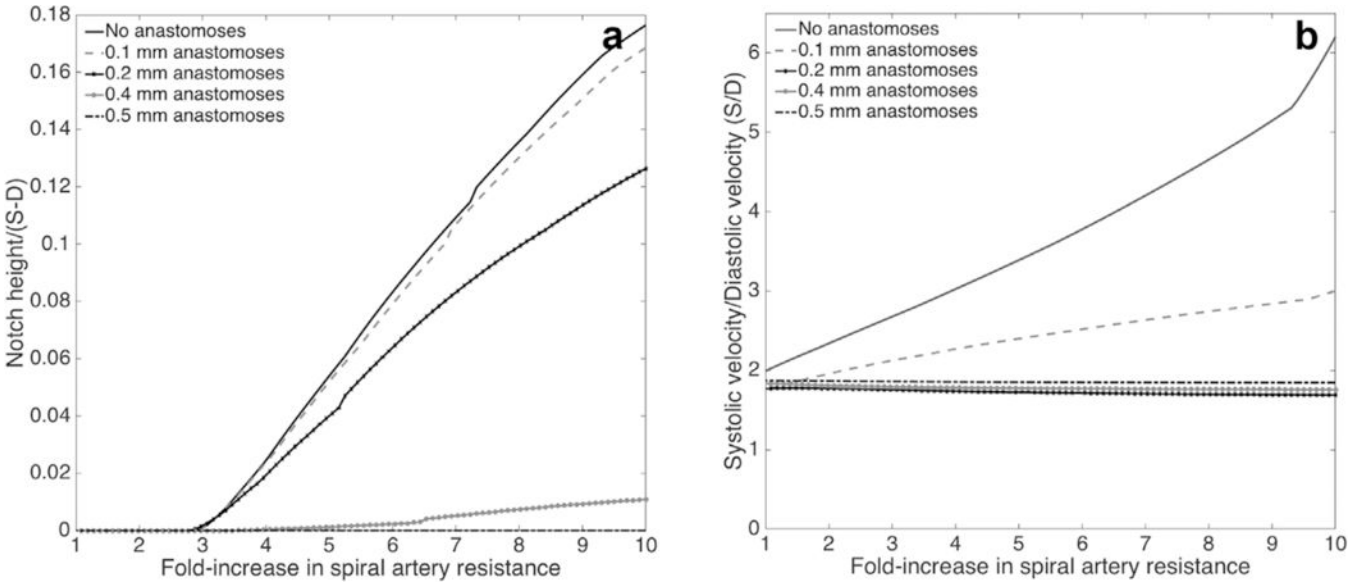

Figure 4:

The predicted relationship between the size of the A-V anastomoses and uterine artery velocity waveform metrics for increasing spiral artery resistance. A) shows the predicted presence of a notch and its height (relative to the height of the velocity waveform. Panels B shows the S/D ratio, and trends in pulsatility index and resistance index are similar. The presence of parallel A-V shunts mitigates the impact of increased placental resistance on each metric and a single 0.4mm radius A-V anastomosis per radial artery is sufficient to produce normal velocity profiles for significant increases in spiral artery resistance

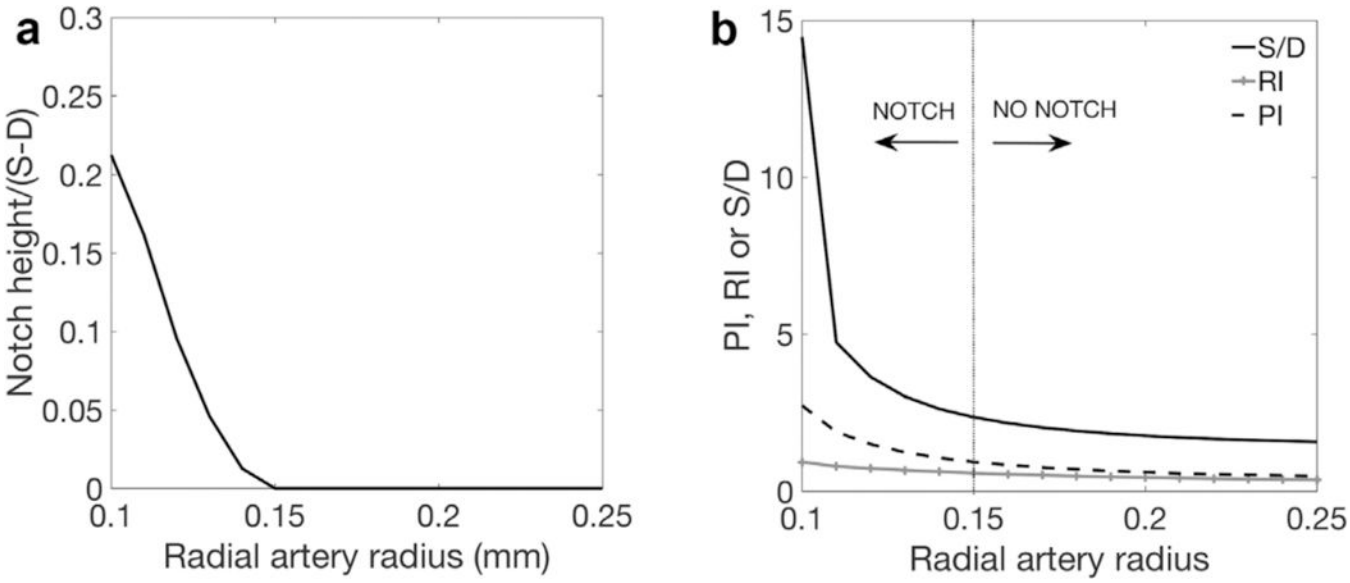

Figure 5:

The predicted relationship between radial artery radius and uterine artery velocity waveforms, with normal spiral artery resistance. Panel A shows the dicrotic notch height, normalized by total height of the velocity waveform and Panel B shows the predicted ratio of systolic (S) to diastolic (D) flow velocity, S/D, resistance index, RI and pulsatility index, PI. There is little impact of radial artery caliber on velocity waveforms over much of the physiological range of radius. However, at radii representative of pre-eclamptic radial arteries, or radial arteries in early pregnancy small changes in radial artery size can result in large changes in uterine artery velocity waveforms.

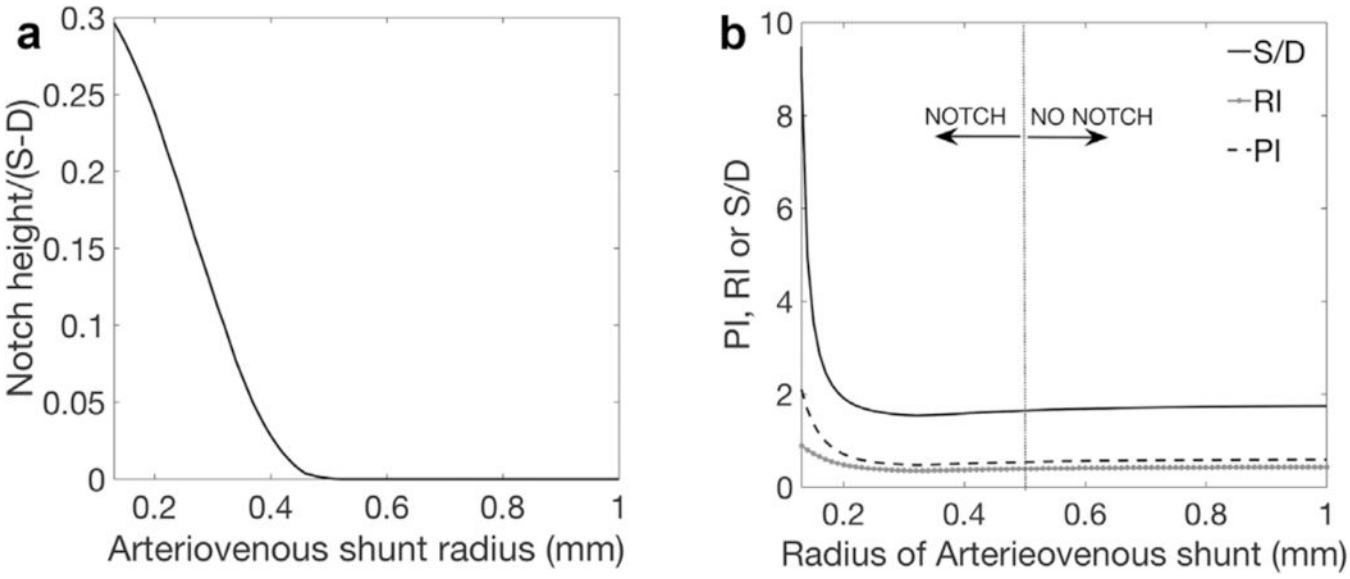

Figure 6:

Model predictions of uterine artery waveform properties when no IVS is present in the model (Model 2). The relationship between A-V shunt radius and notch height (normalized by total waveform height is given in Panel A and the predicted ratio of systolic (S) to diastolic (D) flow velocity, S/D, resistance index, RI, and pulsatility index, PI is given in Panel B. The model shows that if there is a well-established A-V shunt network at term a normal uterine artery waveform is possible. As the A-V shunts, and the rest of the uterine vasculature, decrease in caliber to their pre-pregnancy state during the puerperium the typical non-pregnant 'high resistance' features of the velocity waveform are predicted to return.

Table 1

Model parameters, with ranges and source where available.

Parameter	Value	Reference
Radius of inlet (uterine) artery, r_u	2.0 mm	[10,23]
Length of inlet (uterine) artery, l_u	100 mm	[10,11]
Radius of arcuate artery segment, r_A	Variable, 0.5–4.0 mm	[23]
Length of radial artery segment of arcuate artery, 1_A	18.0 mm	Derived from Ref. [19]
Radius of radial arteries, r_r	0.25 mm	[19,24,26], range 0.1–0.25 mm
Length of radial arteries, l_r	6.0 mm	[28], range 5.0–10.0 mm
Radius of A-V shunts, r_{a-v}	0.2 mm	[27], range 0.1–3.0 mm
Length of A-V shunts, l_{a-v}	9.0 mm	Assumed to be half the distance between two radial arteries (see text)
Young's modulus of uterine arterial walls, E	1.5×10^6 Pa	[11], derived from the internal iliac artery [48]
Vessel wall thickness to vessel radius (h/r_0)	0.1	[11]
Terminal load resistance, R_L	1.60 Pas/mm^3	Derived from total uteroplacental resistance and dimensions of upstream arteries [11]
Terminal load compliance, C_L	1×10^{-8}mm^3/Pa	[11]
Viscosity of blood, μ	3.5×10^{-2}Pas	[11]
Density of blood, ρ	0.105×10^{-2} g/mm^3	[11]
Maternal heart rate	72 bpm	[11]